Original Research

Quantitative Analysis of Whole-Tumor Gd Enhancement Histograms Predicts Malignant Transformation in Low-Grade Gliomas

Paul S. Tofts, PhD,[1]* Christopher E. Benton, DCR,[1] Rimona S. Weil, MA,[1] Daniel J. Tozer, PhD,[1] Daniel R. Altmann, DPhil,[1,2] H. Rolf Jäger, MD,[1] Adam D. Waldman, PhD,[1,3] and Jeremy H. Rees, PhD[1]

Purpose: To quantify subtle gadolinium (Gd) enhancement (signal increase) in whole-tumor histograms and optimize their ability to predict subsequent malignant transformation in low-grade gliomas (LGGs).

Materials and Methods: We analyzed histograms from 21 adult subjects with LGGs (eight nontransformers and 13 transformers) who had been imaged every six months for periods of two to five years. Before transformation these tumors were reported as radiologically non-enhancing. Imaging included a T_1-weighted volume sequence before and after a double dose of Gd-DTPA contrast agent. Image data sets were spatially registered and subtracted to obtain maps of percent enhancement (%E). Tumor outlines were defined on fluid-attenuated inversion recovery (FLAIR) images, and the volumes were calculated. Histogram tails were analyzed to obtain the volume (mL) of subtly enhancing tissue (%E > 10%).

Results: Baseline enhancing volumes were higher for Ts than for NTs ($P < 0.005$). Kaplan-Meier survival curves for a threshold of 4 mL showed clear differences at five years ($P < 0.04$). Pretransformation examinations predicted transformation (corrected threshold = 3.0 mL, $P = 0.011$).

Conclusion: Clear histogram differences at presentation suggest that the process of transformation starts very early. It is now possible to identify individuals at high risk for transformation at baseline by quantifying the volume of subtly enhancing tumor tissue, and such findings could have an impact on patient management.

Key Words: glioma; MRI; Gd enhancement; histogram; transformation; malignancy
J. Magn. Reson. Imaging 2007;25:208–214.

ADULT SUPRATENTORIAL LOW-GRADE GLIOMAS (LGGS) are slow-growing primary brain tumors (WHO grade II) that have a propensity to transform into high-grade gliomas (grades III and IV) after a variable and unpredictable period of time (median = 5–7 years). The majority of patients are young and neurologically intact, and present with a seizure disorder. The initial management of LGG is usually surgical resection, but many of these tumors are diffusely infiltrating and involve areas of eloquent brain function. Early radiotherapy has been shown to prolong time to progression but not overall survival (1); however, in view of concerns about long-term neurotoxicity (2), it is usually reserved for treatment of progressive or recurrent disease. Chemotherapy for oligodendrogliomas, a specific histological subtype of LGG with favorable biological features, is increasingly used as the primary treatment (3), but the long-term benefits are not yet known. Our practice has been to observe such patients with careful clinical and radiological follow-up, to optimize treatment of tumor-associated epilepsy, and to intervene with surgery, chemotherapy, or radiotherapy when there is evidence to suggest tumor progression.

In order to understand better the natural history of tumor progression and the radiological changes that occur over time, we have been scanning newly diagnosed subjects with untreated LGG every six months, using a variety of MR techniques, to determine quantitative parameters that may predict early malignant transformation. The imaging protocol was adapted to incorporate as many techniques as possible within a scan time that is acceptable to patients, and included conventional axial T_2-weighted, sagittal T_1-weighted, and coronal fluid-attenuated inversion recovery (FLAIR) sequences. Additional sequences currently submitted for postprocessing analysis include static perfusion

[1]Institute of Neurology, University College London, London, United Kingdom.
[2]Medical Statistics Unit, London School of Hygiene and Tropical Medicine, London, United Kingdom.
[3]Department of Imaging, Charing Cross Hospital, London, United Kingdom.
Paul S. Tofts' present address is: Brighton and Sussex Medical School, Brighton, UK.
*Address reprint requests to: P.S.T., Brighton and Sussex Medical School, Brighton BN1 9PX, UK.
Received April 13, 2006; Accepted September 7, 2006.
DOI 10.1002/jmri.20800
Published online 30 November 2006 in Wiley InterScience (www.interscience.wiley.com).

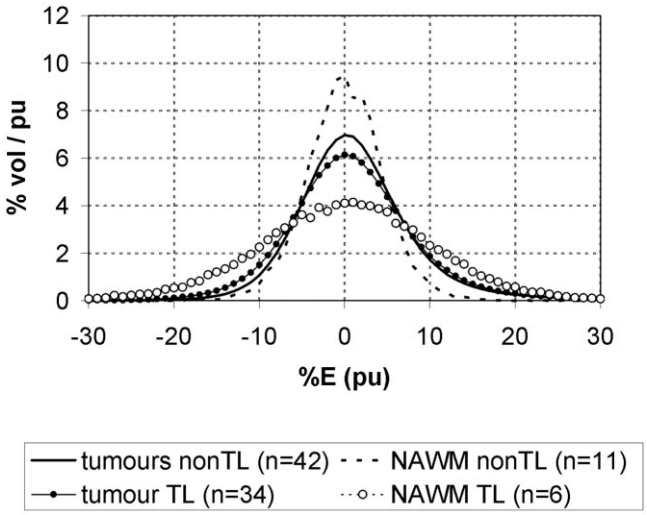

Figure 1. Group mean histograms. Tumors not in a temporal lobe (TL) show increased RH tail. NAWM (non-TL) has a high narrow histogram, reflecting homogeneous tissue composition. Tumors partly or completely in a TL show slightly increased LH tail compared to non-TL, probably caused by TL image artifacts. NAWM completely in a TL is symmetric and has markedly raised tails and reduced PH, probably caused by high image artifact content.

imaging, diffusion-weighted imaging (4), single-voxel short-TE (44 ms) MR spectroscopy (MRS), and thin-slice coronal T_1-weighted volumetric sequences before and after a double dose of Gd contrast agent.

In this work we present a novel method of quantifying subtle Gd enhancement in LGG using difference maps calculated from pre- and post-Gd images. Whole-tumor histograms of subtle (radiologically invisible) enhancement are then constructed from these maps. (The term "enhancement" is used in this paper to denote signal increase, which may not necessarily come from Gd leakage, since small negative enhancements have been observed (see Fig. 6)). It is distinct from "conventional enhancement," which is visible to the naked eye and is reported radiologically. Studies employing histograms (5) have been very successful in quantifying subtle disease in normal-appearing white matter (NAWM) in multiple sclerosis using maps of the magnetization transfer ratio (MTR) (6) and mean diffusivity (7). Several features of interest are extracted from the histograms (e.g., the peak height (PH), peak location (PL), and size of the tails) that give an objective view of the enhancement. Tumor volume is also measured, and hence the volume of tissue (in milliliters) that enhances more than a certain amount (e.g., 10%) can be determined. The correlation of tumor histograms with subsequent tumor behavior (i.e., transformation vs. nontransformation) over the period of follow-up is then examined, and the predictive ability of the histograms is calculated.

MATERIALS AND METHODS

A total of 21 subjects (nine nontransformers (NTs) and 12 transformers (Ts)) were analyzed in this pilot study. The subjects were selected from a larger database of about 60 subjects who had been scanned. Since the analysis was time-consuming, not all subjects could be analyzed in this pilot study. The groups were chosen to use all of the Ts, and to obtain approximately equal numbers in each group. Two NTs had biopsy-proven oligodendrogliomas, four had astrocytomas, and three were not biopsied. Of the Ts, two had oligodendrogliomas, eight had astrocytomas, and two had mixed gliomas comprising both astrocytic and oligodendroglial elements (Table 1). The study was approved by the joint ethics committee of our hospital and institute, and the patients gave informed consent.

Serial scanning was carried out every six months and ceased if transformation took place. Transformation was defined as clinical deterioration (the appearance of a progressive neurological deficit or raised intracranial pressure) or radiological progression (the appearance of new or increased conventional (visible) enhancement).

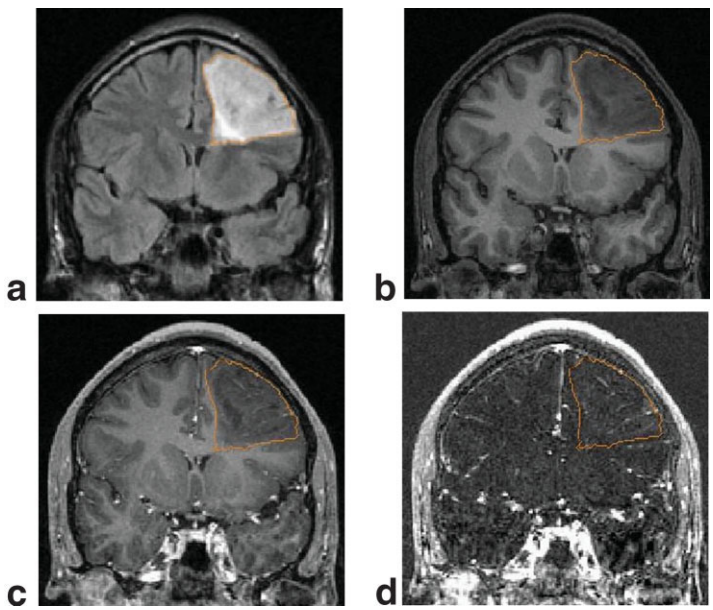

Figure 2. Example cropped images from a tumor immediately before transformation: (**a**, top left) FLAIR, (**b**) pre-Gd T1-w SPGRE, (**c**) post-Gd, and (**d**, bottom right) %E map (range = –20 to +60 pu). Note the lack of visible (conventional) enhancement.

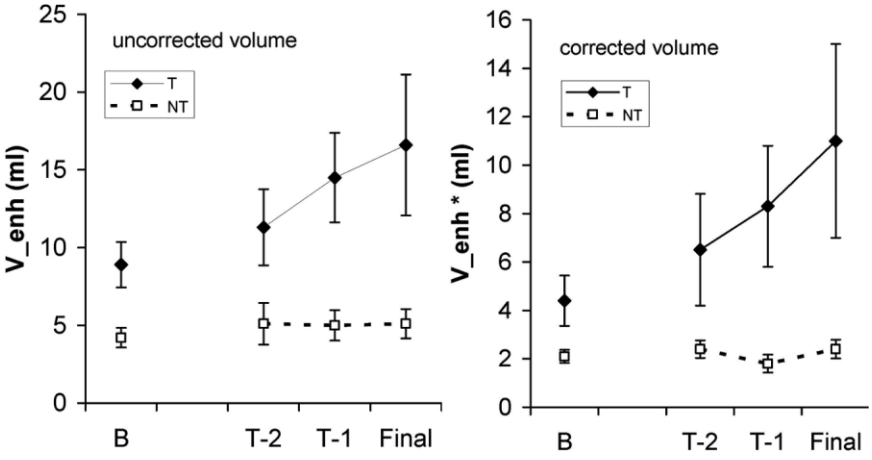

Figure 3. Serial change in the volume of enhancing tissue (mean and standard error (SE)). Note the clear group difference at baseline (B, the entry examination), the stability of the NTs, and the steady progression in the Ts. For the Ts, transformation took place at a time between T_{-1} and the final scan. Uncorrected volume V_{enh} is shown in LH plot. Note the reduced SEs in NTs when the corrected volume V_{enh}* (RH plot) is used compared to the uncorrected volume.

Suspected progression was confirmed by biopsy of the enhancing region or resection of the tumor. Most subjects had their first (baseline) scan within two years of presentation of symptoms (median time from first seizure to baseline scan = 10 months; range = 3–66 months). The subjects were followed for an average of five scans (range = 2–7). The time between first seizure and the penultimate scan (NT_{-1} or T_{-1} (see below)) was not significantly different between the two groups.

The MRI examinations consisted of two sequences. Fast spin-echo (FSE) FLAIR imaging (which is low-resolution) was carried out to define the tumor boundaries. The imaging parameters were TR/TI/TE = 8774/2192/161 msec; pixel size = 0.94 × 0.94 mm; slice thickness = 5 mm; and gap = 1.5 mm. Three-dimensional (3D) T_1-weighted IR spoiled gradient-echo (SPGRE) images (high-resolution volume images) were collected before and 10 minutes after injection of a double dose of Gd contrast agent (Dotarem 0.2 mmole/kg). The parameters were TR/TI/TE = 14.4/650/6.4 msec; flip angle (FA) = 20°; and voxel size = 0.94 × 0.94 × 1.5 mm. The scanner gain settings were kept fixed during each examination (with the exception of a few early examinations before the procedure was stabilized).

The 3D image data sets were spatially registered (8) and subtracted using software developed in-house. Contralateral NAWM signal intensity was measured in both pre- and post-Gd images, always keeping the same location in each patient. Maps of percentage enhancement (%E) were calculated from %E = 100*(image difference)/(mean NAWM value) in terms of percent units (pu). The mean NAWM value was derived from the average of the pre- and post-Gd values to reduce noise.

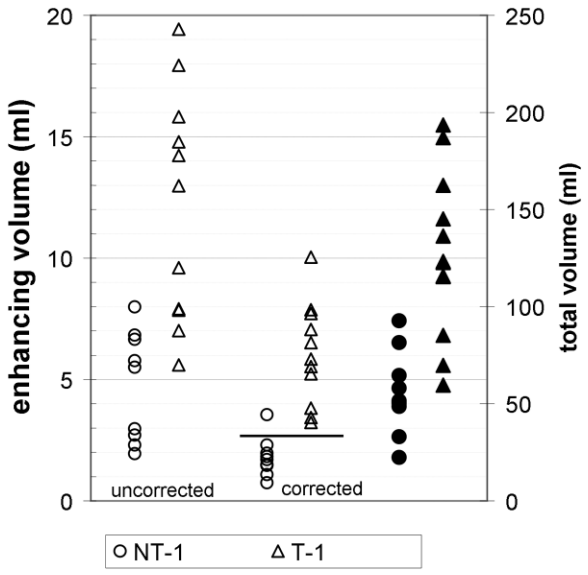

Figure 4. Scatterplot of individual values of enhancing volume in the penultimate examination. Ts (T_{-1}) transformed in the next six months, while NTs (NT_{-1}) did not. Using the corrected volume V_{enh}* gives almost complete separation of the two groups. A volume threshold of V_{enh}* > 2.8 mL (solid bar) detects all those who will transform within the next six months, with only one false positive. Note the reduced scatter within the NT_{-1} group when the corrected volume is used compared to the uncorrected volume. One T subject with enhancing volumes >30 mL is not shown. The total tumor volume (RHS of figure, solid symbols) gives less good discrimination between NT_{-1} and T_{-1}.

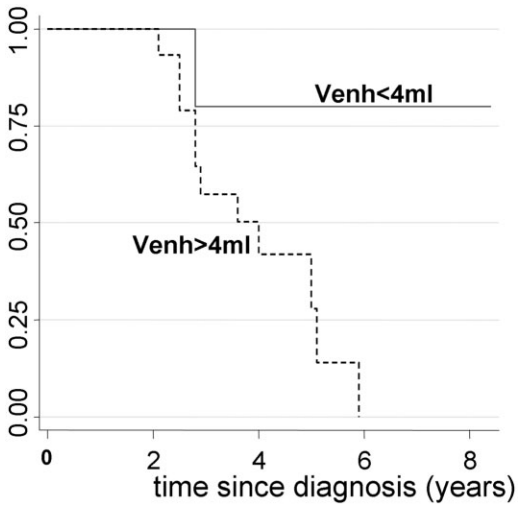

Figure 5. Kaplan-Meier graph using the uncorrected enhancing volume, showing the proportions of subjects who survived untransformed over the follow-up period from diagnosis in the V_{enh} < 4 mL and V_{enh} ≥ 4 mL groups (P = 0.039).

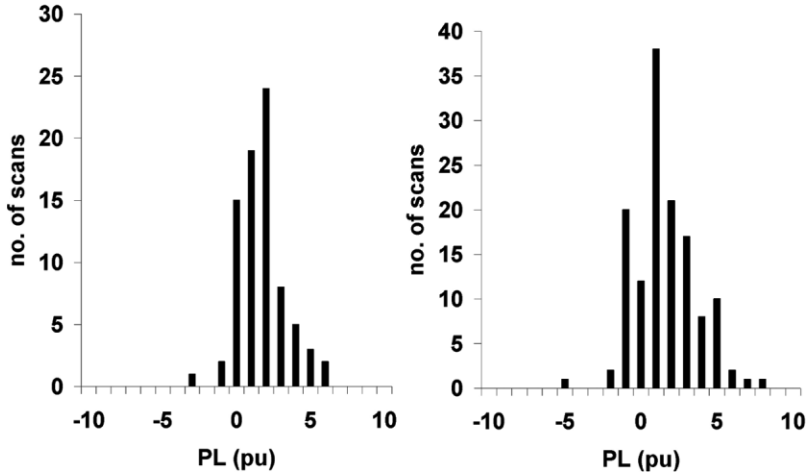

Figure 6. PL histograms (left: without NAWM correction; right: with NAWM correction). Some PL values are negative, probably due to scanner instability, and therefore all histograms were shifted to have PL = 0.

The low-resolution (6.5-mm slice separation) 2D FLAIR images were interpolated (to 1.5-mm contiguous slices) and then registered to the pre-Gd high-resolution 3D T_1-weighted data set (9). The tumors were outlined as regions of interest (ROIs) on the interpolated FLAIR images (which give the best tumor contrast) using the semiautomated contour method in DispImage (10,11). These ROIs were then copied to the %E maps. NAWM ROI sets were also generated in both the temporal lobes (TLs) and elsewhere for quality control.

A histogram of %E within each tumor was then produced (5). This was normalized to a total tumor volume of 100%. The bin width was 1 pu. Random noise was added to the pre- and post-Gd images to avoid spikes in the resulting histogram (12).

Six primary features were extracted from the histograms: 1) PH, 2) PL, 3) mean, 4) R% (the size of the right-hand (RH) tail beyond 10 pu, i.e., the tumor volume fraction that enhanced more than 10 pu), 5) L% (the size of the left-hand (LH) tail, below –10 pu), and 6) skew (a measure of how asymmetric the histogram was). The PL was found to be unreliable (see results below), and therefore the histograms were shifted until the peak was at 0 pu before the three last parameters (R%, L%, and skew) were calculated.

The volume of each tumor was measured from the interpolated FLAIR image ROIs. Phantom measurements have shown that these volumes are accurate and reproducible (unpublished data). Two secondary parameters (V_{enh} and V_{enh}*) were calculated from the volume. V_{enh} is the absolute volume of tumor (mL) that enhanced more than 10 pu (V_{enh} = R%*volume). V_{enh}* was calculated using the *difference* of the RH and LH tails (since some subjects had unusually high LH tails

Table 1
Patient Characteristics

Nontransformer/ transformer	Age	Gender	Time to first scan (months)	Time to transformation	Histology
NT1	63	F	9		O
NT2	26	M	66		
NT3	45	F	4		O
NT4	29	F	29		A
NT5	42	M	6		A
NT6	54	M	12		
NT7	33	M	5		
NT8	39	M	35		A
NT9	29	M	2		A
T1	30	F	15	33	O
T2	57	M	17	35	O
T3	38	M	8	33	AA
T4	31	M	9	27	AA
T5	41	M	43	61	GA
T6	47	F	40	71	AA
T7	35	M	31	60	GBM
T8	65	F	6	48	AOA
T9	30	M	18	30	GBM
T10	30	M	9	33	AA
T11	29	F	7	31	AA
T12	24	M	6	30	AO

A = astrocytoma, AA = anaplastic astrocytoma, O = oligodendroglioma, GA = gemistocytic astrocytoma, GBM = glioblastoma multiforme, AO = anaplastic oligodendroglioma.

(see below)). Thus V_{enh}* = (R% – L%)*volume. In principle the histogram normalization procedure was unnecessary, since the histograms were then multiplied by absolute volume (in milliliters); however, the normalized histograms provide a convenient way to compare visually tumors of different sizes.

We compared the features of the T and NT groups using *t*-tests. Scatter plots were used to examine the possibility of predicting transformation for individual subjects. The baseline scans of those who remained NT (NT_0) were compared with those of subjects who transformed later in the study (T_0). Features from the last scan before transformation (T_{-1}) and the scan immediately after transformation occurred (T_{+1}) were compared with those from NTs. For NTs we used the penultimate scan NT_{-1}, since the last NT scan could in fact be a T_{-1} if the subject was subsequently shown to transform. This analysis indicates the likelihood of being able to predict transformation in the six-month period following a scan. The scan immediately before T_{-1} (i.e., T_{-2}) was also examined to look for signs of change in the period leading up to transformation.

A survival analysis using the baseline scans was also undertaken. A binary threshold for V_{enh} was chosen at 4 mL. This threshold gave the highest proportion of patients correctly classified as transforming/not transforming during follow-up, and was also the median in the NT group. The binary variable $V_{enh} \geq 4$ mL vs. $V_{enh} <$ 4 mL was then used to define the two groups for a Kaplan-Meier plot, which estimates and plots the proportion of NT patients at any given time since diagnosis during the follow-up period, and for a log rank test, which tests the difference in this proportion between the two groups over the whole follow-up period.

RESULTS

The group mean histograms in Fig. 1 show the general properties of each tissue type. Tumors not in a TL show increased RH tail. NAWM (non-TL) has a high narrow histogram, reflecting homogeneous tissue composition. Tumors partly or completely in a TL show slightly increased LH tail compared to non-TL tumors, probably caused by TL image artifacts. NAWM completely in a TL is symmetric and has markedly raised tails and reduced PH, probably caused by high image artifact content. A typical set of images from one slice is shown in Fig. 2.

In group comparisons, the skew parameter and PH showed very little significance, and both were dropped. The most successful were V_{enh}, the volume of enhancing tissue calculated from the RH tail, and V_{enh}*, the volume of enhancing tissue after correction for the LH tail (Fig. 3).

At baseline the T_0 scans already had significantly higher volumes of enhancing tumor tissue than the NT_0 scans (one-tailed *t*-test, unequal variance; V_{enh}: $P <$ 0.004; V_{enh}*: $P = 0.02$).

Transformers (i.e., those who were seen to transform during this study) progressed steadily from their first exam. Thus the T_{-2} exams revealed higher volumes of enhancing tissue than baseline (one-tailed paired *t*-test, V_{enh}: $P < 0.006$, V_{enh}*: $P < 0.03$), and T_{-1} exams revealed higher volumes of enhancing tissue than the T_{-2} exams (one-tailed paired *t*-test; V_{enh}: $P < 0.02$; V_{enh}*: $P < 0.01$).

The pretransformation volumes T_{-1} were very different from the NT_{-1} volumes (Fig. 4; one-tailed *t*-test, unequal variance; V_{enh}: $P < 0.003$; V_{enh}*: $P < 0.01$). The T_{-1} volumes could be distinguished in all but one case from NT_{-1} scans (corrected volume V_{enh}*; Fig. 4) using a threshold of 2.8 mL for V_{enh}*. The total tumor volume and the uncorrected enhancing volume V_{enh} both performed less well (Fig. 4).

The Kaplan-Meier plot for uncorrected volumes in Fig. 5 shows that the $V_{enh} < 4$ mL group had a substantially higher probability of remaining untransformed during the period after three years from diagnosis than the $V_{enh} \geq 4$ mL group. For example, the estimated probability of untransformed survival to five years is 0.80 (95% confidence interval (CI) = 0.20, 0.97) in the <4 mL group compared to 0.28 (95% CI = 0.06, 0.56) in the ≥4 mL group. The log rank test, which globally tests the difference in such proportions over all the time points, gives $P = 0.039$. Plots of the corrected volume V_{enh}* did not produce markedly better results.

The PL values of the histograms varied in an unexpected way (see Fig. 6a). Some values were negative, while a true negative enhancement after Gd injection is extremely unlikely. The most likely cause was a small unexpected change in MR imager gain between the two volume image data sets. The signal intensity in NAWM was measured and used to normalize the signal intensity in the second image data set. Although this reduced the range of PL values slightly (Fig. 6b), some values were still implausible. We concluded that the PL values were not meaningful, and that all histograms should be shifted until the peak lay at 0 pu. Similarly, the mean was discarded as a parameter. We then measured the size of the tails using thresholds (±10 pu) defined with respect to the PL, and these parameters were insensitive to any changes in imager gain.

Inspection of the tumor histograms showed that the size of the LH tail (below –10 pu) varied considerably. It was often larger than that seen in most NAWM, and probably more than can be explained by image noise (see Fig. 1). A significant number of voxels having a genuine negative enhancement as a result of injection of Gd is very hard to explain. We hypothesized that image artifacts, particularly in the TL, could be the cause. Tumors were classified as being either completely, partially, or not at all in the TL. A basic image quality scoring system was set up, and one image data set for each patient was scored. TL slices had more artifact than those from elsewhere, particularly after Gd injection.

The relationship between the location of a NAWM set of ROIs and the size of its left histogram tail was examined. Locations were categorized as non-TL, partial, or TL. The mean LH tail increase was consistent with a linear relationship, estimated to increase by 1.8 %vol per category change toward temporal (95% CI = 0.7, 2.8; $P = 0.003$ in a test of linear trend). This can also be seen in Fig. 1: regions not in a TL had the lowest LH tails, and regions in TLs had the highest tails.

These data all support the concept that high LH tails in NAWM are associated with the TLs and are probably related to increased artifact in that location. Thus, improved imaging techniques might reduce the LH tail sizes. This concept encouraged us to explore the difference between the RH and LH tails as a more reliable parameter than the RH tail alone to characterize genuine Gd leakage (see Fig. 4).

DISCUSSION

This study presents the first prospective evaluation of patterns of Gd enhancement in untreated LGGs and shows clear histogram differences between tumors that subsequently transformed in the period under study and those that did not (Figs. 3–5). By analyzing images pre- and post-Gd, one can now obtain objective quantification of abnormal subtle enhancement, even at baseline, and predict with a high degree of precision the likelihood of subsequent transformation. As a new technology, this method looks very promising as a means of identifying patients who should be treated earlier rather than later. Histograms from patients who were about to transform were clearly distinguishable from those who were not (Fig. 5). Using a threshold of $V_{enh}^* > 2.8$ mL, all subjects who were about to transform were detected, with only one false-positive out of the nine nontransformers (i.e., sensitivity = 100%, specificity = 89%). Conversely, a patient with $V_{enh}^* < 2.8$ mL is unlikely to transform in the next six months, and this information can be used to provide reassurance to the patient.

We derived two volumes (an uncorrected volume, V_{enh}, and a corrected volume, V_{enh}^*) based on subtraction of the LH tail from the RH tail. The latter has a logical basis in that in principle it is independent of any image noise or artifact (which might be expected to have a symmetric effect on the histogram). It provides a better classification of the two groups (NT and T), pretransformation (Fig. 4), and a lower NT standard deviation (see Fig. 3). V_{enh} would appear to be a better parameter judging by the *t*-test ($P < 0.003$ vs. $P < 0.01$), and this demonstrates the importance of looking at classification performance when evaluating a parameter for clinical management of individual patients.

The significance of the increased LH tail is not yet completely clear; however, further study may enable variation from this source to be reduced, yielding improvements in classification performance. A small amount of negative enhancement could be caused by intravascular Gd reducing the T_2^*. Approximate calculations indicate a magnitude of 2–3 pu. This may make a contribution to the negative tails observed (see Fig. 1); however, the symmetric increases in tail size beyond −10 pu and +10 pu in TL NAWM are almost certainly caused by other factors. The loss of absolute PL information is regrettable, since without this information any sensitivity to uniform enhancement is lost. However, our experiments show that the scanner instability can reach 2% or possibly more, which sets a limit to the smallest absolute PL change that could be measured. The consistent behavior of our extracted parameters Venh and V_{enh}^* (Fig. 3) gives us confidence in their reliability. We believe they are relatively insensitive to scanner drift, noise, and artifact.

The enhancement parameter %E used in this study is unusual. Usually signal change is measured as a fraction of pre-Gd tumor value, and here we measured it as a fraction of the NAWM value. This has two benefits. First, NAWM can be better characterized because it is homogeneous, and a large ROI can be drawn, reducing the effect of noise. Second, in a highly T_1-weighted SPGRE sequence ($TR \ll T_1$), simple modeling shows that $\%E = (PD^{tumor}/PD^{NAWM})*(\Delta R_1{}^{tumor}/R_1{}^{NAWM})$, where $R_1 = 1/T_1$ and $\Delta R_1{}^{tumor}$ is the change in R_1 brought about after injection of Gd. Thus the signal change is independent of the initial tumor T_1 value, and the potential confounding effect of tumor T_1 is removed. PD^{tumor} is likely to be raised above PD^{NAWM} by the presence of edema, and NT tumors may differ slightly from T tumors. The effect is unlikely to be large, since otherwise T_1 would be a successful discriminator between NT and T. Any difference would in turn slightly alter the scaling factor between $\Delta R_1{}^{tumor}$ and the measured %E, and hence in principle could make a small contribution to the observed differences between NT and T. Direct measurements of PD, or estimated measurements using PD-weighted images, would resolve this issue.

The standard deviation (SD) values in the NT group were consistently lower than in the T group (see Fig. 3), particularly when the corrected values of enhancing volume were used. This supports the notion that the NT group is relatively homogeneous and stable, and differs from the rather more heterogeneous T group.

The differences seen at baseline between NT and T (Figs. 3 and 5) suggest that the process of transformation begins several years before it is apparent by more conventional radiological imaging criteria. Refinement of the quantitative MR examination may enable this difference to be made even more obvious. This prognostic information could in turn alter patient management, and the MR information could be used to evaluate the success of pretransformation treatment.

This paradigm circumvents the problem inherent in the T/NT approach, i.e., that initially all "Ts" are NTs, and after a long time most "NTs" will transform. The distinction between the groups is that Ts transform relatively soon (within the length of this study), while NTs transform much later (longer than this study).

With a larger data set that includes more Ts, improved analysis methods may be possible. Feature extraction could include looking at thresholds other than 10% enhancement (this was chosen on the basis of the NAWM histograms, which are almost zero at 10 pu (see Fig. 1)); however, it is unlikely to be optimal. Previous studies have used discriminant analysis to extract optimum features from histograms (13). There is some evidence that glioma subtypes (astrocytomas and oligodendrogliomas) behave differently, and certainly they have different diffusion characteristics (4). One could perhaps make the survival analysis a continuous function of the baseline V_{enh}^*, instead of forcing the parameter into one of two categories with a threshold. The approach could be refined to include information from each examination (instead of just the first one,

as in Fig. 5) giving an updated prognosis at each patient visit. Several other MR parameters (e.g., diffusion) were measured on these subjects, and multiparametric statistical modeling (including rates of change) may improve prediction. The enhancement is clearly localized within the tumor (otherwise the histograms would not develop tails), and it would be interesting to study its location and possible texture.

As the prediction system becomes better trained using unequivocal subjects, it could be used to aid management in equivocal subjects. For example, if it is unclear whether transformation has taken place, a large value for V_{enh}* would add support to the idea that it has.

In conclusion, we describe a quantitative method for analyzing subtle Gd enhancement in LGGs, and show that there is a clear difference between NTs and Ts even at baseline, i.e., years before conventional techniques can detect enhancement.

REFERENCES

1. van den Bent MJ, Afra D, de WO, et al. Long-term efficacy of early versus delayed radiotherapy for low-grade astrocytoma and oligodendroglioma in adults: the EORTC 22845 randomised trial. Lancet 2005;366:985–990.
2. Klein M, Heimans JJ, Aaronson NK, et al. [Impaired cognitive functioning in low-grade glioma patients: relationship to tumor localisation, radiotherapy and the use of anticonvulsants]. Ned Tijdschr Geneeskd 2004;148:2175–2180.
3. Stege EM, Kros JM, de Bruin HG, et al. Successful treatment of low-grade oligodendroglial tumors with a chemotherapy regimen of procarbazine, lomustine, and vincristine. Cancer 2005;103:802–809.
4. Tozer DJ, Jager HR, Danchaivijitr N, Benton CE, Tofts PS, Rees JH, Waldman AD. Apparent diffusion coefficient histograms may predict low-grade glioma subtype. NMR Biomed. 2006 in press. DOI: 10.1002/nbm.1091.
5. Tofts PS, Davies GR, Dehmeshki J. Histograms: measuring subtle diffuse disease. In: Paul Tofts, editor. Quantitative MRI of the brain: measuring changes caused by disease. Chichester: John Wiley; 2003. p 581–610.
6. van Buchem MA, McGowan JC, Kolson DL, Polansky M, Grossman RI. Quantitative volumetric magnetization transfer analysis in multiple sclerosis: estimation of macroscopic and microscopic disease burden. Magn Reson Med 1996;36:632–636.
7. Cercignani M, Iannucci G, Rocca MA, Comi G, Horsfield MA, Filippi M. Pathologic damage in MS assessed by diffusion-weighted and magnetization transfer MRI. Neurology 2000;54:1139–1144.
8. Woods RP, Cherry SR, Mazziotta JC. Rapid automated algorithm for aligning and reslicing PET images. J Comput Assist Tomogr 1992; 16:620–633.
9. Studholme C, Hill DLG, Hawkes DJ. An overlap invariant entropy measure of 3D medical image alignment. Patt Recognit 1999;32: 71–86.
10. Plummer DL. DispImage a display and analysis tool for medical images. Rivista Neuroradiol 1992;5:489–495.
11. Grimaud J, Lai M, Thorpe J, et al. Quantification of MRI lesion load in multiple sclerosis: a comparison of three computer-assisted techniques. Magn Reson Imaging 1996;14:495–505.
12. Tozer DJ, Tofts PS. Removing spikes caused by quantization noise from high-resolution histograms. Magn Reson Med 2003;50:649–653.
13. Dehmeshki J, Ruto AC, Arridge S, Silver NC, Miller DH, Tofts PS. Analysis of MTR histograms in multiple sclerosis using principal components and multiple discriminant analysis. Magn Reson Med 2001;46:600–609.